JOC The Journal of Organic Chemistry

Article

pubs.acs.org/joc

Chemical Reactivity of Alkenes and Alkynes As Seen from Activation Energies, Enthalpies of Protonation, and Carbon 1s Ionization Energies

Alf Holme,[†] Leif J. Sæthre,*[,†] Knut J. Børve,[†] and T. Darrah Thomas[‡]

[†]Department of Chemistry, University of Bergen, NO-5007 Bergen, Norway, and

[‡]Department of Chemistry, Oregon State University, Corvallis, Oregon 97331-4003, United States

Supporting Information

ABSTRACT: Electrophilic addition to multiple carbon−carbon bonds has been investigated for a series of twelve aliphatic and aromatic alkenes and the corresponding alkynes. For all molecules, enthalpies of protonation and activation energies for HCl addition across the multiple bonds have been calculated. Considering the protonation process as a cationic limiting case of electrophilic addition, the sets of protonation enthalpies and gas-phase activation energies allow for direct comparison between double- and triple-bond reactivities in both ionic and dipolar electrophilic reactions. The results from these model reactions show that the alkenes have similar or slightly lower enthalpies of protonation, but have consistently lower activation energies than do the alkynes. These findings are compared with results from high resolution carbon 1s photoelectron spectra measured in the gas phase, where the contribution from carbons of the unsaturated bonds are identified. Linear correlations are found for both protonation and activation energies as functions of carbon 1s energies. However, there are deviations from the lines that reflect differences between the three processes. Finally, substituent effects for alkenes and alkynes are compared using both activation and carbon 1s ionization energies.

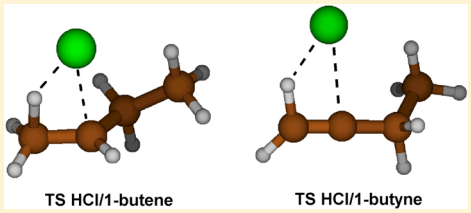

1. INTRODUCTION

Electrophilic addition to carbon−carbon multiple bonds is one of the most common and useful reaction types in organic chemistry, and a wealth of experimental and theoretical information has been gathered over the years. A recurrent question has been that of the relative chemical reactivity of carbon−carbon double and triple bonds in proton addition reactions.[1−3] In general, alkynes are regarded as somewhat less reactive than alkenes.[1] However, structurally similar alkenes and alkynes have rate constants of the same magnitude in acid-catalyzed hydration reactions and gas-phase proton additions.[3−6] Another trend to emerge from these early studies is that the reactivity of the triple bond may be more affected by substitution in the α position than is the double bond.[3,7]

The relative reactivity of the double and triple bonds may depend on reaction conditions such as the choice of solvent and the electrophile. A useful set of rate constants for acid-catalyzed hydration reactions of alkynes and alkenes, obtained under similar conditions, is found in ref 7. A subset of the data is shown in Figure 1a, and one may note that the alkene and alkyne reactivities appear to be quite similar. The short-chained members of the series make exceptions to this trend, and it is suggested in ref 7 that this may be due to specific solvent interaction for these alkynes. In order to be free of such solvent effects it is useful to consider reactions in the gas phase rather than in solution.

Earlier studies have shown that valence ionization energies (VIEs) and reaction rates in electrophilic addition reactions are related quantities.[9−12] It is therefore reasonable to assume that VIEs provide an indication of the relative reactivity of alkenes and alkynes in these reactions. It is apparent from Figure 1b that the alkenes have systematically lower VIEs than the alkynes. If VIEs reflect relative reactivities in proton addition reactions, the alkenes should be more reactive than the alkynes for such reactions, but this is not reflected in the reactivity data in Figure 1a. While valence ionization energies measure the energy cost of extracting a π electron from the unsaturated bond, the reaction rate is affected by other important factors not reflected in an ionization energy, such as steric repulsion, the stabilizing energy of forming a partial bond to the electrophile, and solvent interactions.

In solution, the kinetics of many electrophilic addition reactions is consistent with a two-step mechanism involving slow attack by an ionic electrophile followed by neutralization. In the specific case of the hydration of ethyne, this mechanism may be formulated as follows:

$$\mathrm{HCCH} + \mathrm{H_3O^+} \xrightarrow{\text{slow}} \mathrm{H_2C{=}CH^+} + \mathrm{H_2O} \xrightarrow{\text{fast}} \text{products} \quad (1)$$

For both ethyne and the analogous case of ethene, the formation of a carbocation is believed to be the rate-determining step. Hence, the ability of the molecule to accept a positive charge is decisive for the rate of the overall reaction.

Received: August 2, 2012
Published: October 10, 2012

dx.doi.org/10.1021/jo301627d | J. Org. Chem. 2012, 77, 10105−10117

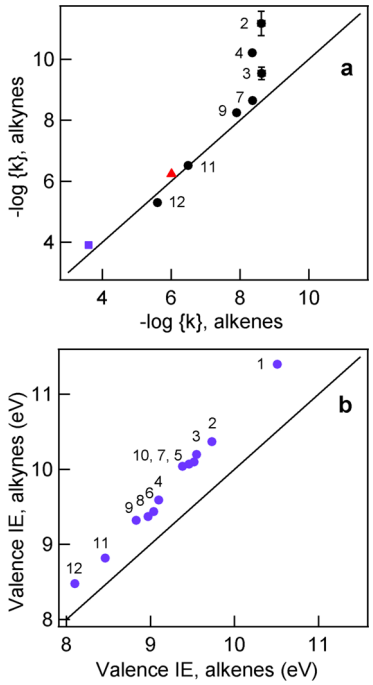

Figure 1. The $-\log\{k\}$ values for acid-catalyzed hydration reactions[7] (top) and valence ionization energies[8] (bottom) of alkynes plotted against the corresponding alkene values. Here, $\{k\}$ is the numerical value of k in units of $M^{-1}s^{-1}$. In the top figure, the 3-methylstyrene/3-ethynyltoluene data point is shown with a red triangle, and the ethenylcyclopropane/ethynylcyclopropane point with a blue square (not included in our list of twelve alkyne/alkene pairs in Table 1). Straight 1:1 lines are included to guide the eye. See text and Supporting Information for details, and Table 1 for identification of each alkyne/alkene pair.

This suggests that the proton affinity might be useful as a predictor of reactivity, as it takes into account both the energy cost of extracting π electrons and the stabilizing effect of forming the new C−H bond.

A related process is carbon 1s ionization, which also involves creating a positive charge at a specific site in the molecule. This similarity is illustrated in Scheme 1, with proton addition in (**a**) and core ionization in (**b**) where the core-ionized carbon, which is a radical with an unpaired electron in the C1s orbital, is marked with an asterix.

Scheme 1

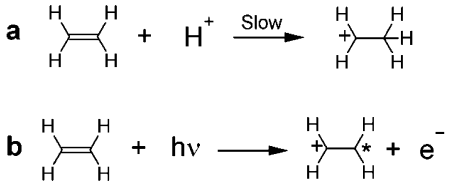

In the X-ray photoelectric event, π electrons are relocated to screen the ionized carbon rather than forming a new σ bond. Nonetheless, for molecules with double bonds and also for methyl-substituted benzenes, a close relationship has been observed between core-ionization energies and activation energies of electrophilic addition reactions.[13−15]

In this work, we explore the relative reactivity of carbon−carbon double and triple bonds by comparing reactivities of alkenes with the analogous alkynes in model electrophilic addition reactions. To this end, we have selected twelve pairs of aliphatic and aromatic alkenes and alkynes as listed in Table 1. Among these compounds are pairs that display the unsaturated bonds in terminal positions as well as those that possess the functional groups in internal (or nonterminal) positions.

Table 1. Alkenes and Corresponding Alkynes Studied in This Work

ID[a]	alkene	alkyne
1	ethene	ethyne
2	propene	propyne
3	1-butene	1-butyne
4	*trans*-2-butene	2-butyne
5	1-pentene	1-pentyne
6	*trans*-2-pentene	2-pentyne
7	1-hexene	1-hexyne
8	*trans*-2-hexene	2-hexyne
9	*trans*-3-hexene	3-hexyne
10	1-heptene	1-heptyne
11	styrene	ethynylbenzene
12	4-methylstyrene	4-ethynyltoluene

[a]Identification number of each pair used to label the associated data entry in figures.

In order to obtain a uniform set of reactivity data without solvent effects, we use theoretical calculations of gas-phase activation energies for the model reaction of HCl addition to each of the molecules appearing in Table 1. Addition of hydrogen halides to alkenes and alkynes has traditionally served as a paradigm for electrophilic addition to unsaturated systems.[2,16] The transition states may be characterized as having a four-center structure, implying that the electrophilic attack and the nucleophilic step take place in a concerted but not necessarily symmetric way. In contrast, in solution the rate-determining step in many electrophilic addition reactions consists of attack by an ionic electrophile, thus displaying a much higher degree of ionicity than that found in the gas phase. We will consider protonation to represent a gas-phase model for the rate-determining electrophilic attack in solution, and we prepare a set of enthalpies of protonation to the carbons involved in double and triple bonds by a highly accurate quantum chemical compound method. The sets of gas-phase activation energies and protonation enthalpies allow for direct comparison between double and triple bond reactivities in both dipolar and ionic electrophilic reactions. Moreover, we aim for additional insight by constructing a parallel data set of experimental carbon 1s ionization energies, as this method offers local probing of all unique carbon atoms in the molecules, thus throwing light also on reasons for inactivity as well as reactivity. Site-specific C1s energies have become available only in recent years, through a combination of very bright radiation at third-generation synchrotron facilities, high-resolution electron energy analyzers, and the development of theoretical tools for detailed analysis of complex photoelectron spectra. The latter aspect is particularly useful for some of the rather large molecules where the separation of ionization energies is small and possibly affected by the presence of several conformers.[17−20] It may be noted that the relationship between C1s ionization energies, proton affinities and activation energies in electrophilic reactions to alkynes has not been explored before.

dx.doi.org/10.1021/jo301627d | J. Org. Chem. 2012, 77, 10105−10117

2. COMPUTATIONAL DETAILS

For the optimization of transition-state structures and calculation of activation energies, density functional theory was used with the B3LYP exchange-correlation functional as implemented in Gaussian03.[21] Saturated parts of the hydrocarbons were described with atom-centered Gaussian-type functions contracted to triple-ζ quality as described by Dunning[22] and augmented by polarization functions,[23] leading to C: [5s, 3p, 1d] and H: [3s, 1p]. In this work, this is referred to as the TZP basis. For the unsaturated carbon atoms, this set was augmented by diffuse s,p functions with exponents α_s = 0.04561 and α_p= 0.03344. Similarly, HCl was described by H: TZP + diffuse s function (α_s = 0.0709); Cl: McLean-Chandler [6s,5p][24] plus diffuse even-tempered sets of s and p functions (α_s = 0.0600; α_p = 0.0314) and a doubly split polarization set. All polarization functions were taken from Pople,[23] either "6-311G(2d)" (Cl) or "6-311G(d,p)" (C, H).

For the computation of enthalpies of protonation at 298.15 K, the G3 compound method[25] was used. All theoretical models used for analysis of X-ray photoelectron spectra are given in Appendix A.2.

3. RESULTS AND DISCUSSION

This section is organized as follows. First, gas-phase addition of HCl to the alkenes and alkynes listed in Table 1 is explored by quantum chemistry using density functional theory. Transition-state geometries are optimized and activation energies calculated. Next, enthalpies of protonation are obtained for the full set of molecules. From the result of both of these model reactions, the relative reactivities of alkenes and alkynes are compared.

Experimental carbon 1s ionization energies (C1s IE) are obtained for all carbon atoms in the molecules under study by detailed analysis of high-resolution C1s photoelectron spectra. We explore to what extent chemical shifts in C1s energies reflect the variation in protonation energies within series of alkynes and alkenes, and between structurally related alkynes and alkenes. Next, trends in activation energies are analyzed by comparison to chemical shifts in C1s ionization energies.

Finally, substituent effects are explored from activation energies and C1s ionization energies. To this end, linear additivity models have been calculated to investigate the effect of the individual substituents.

3.1. Activation Energies (E_a) in HCl Addition Reactions. Activation energies in the gas phase are not readily available but may be obtained from theoretical calculations. Calculated activation energies for the addition of HCl have been reported previously for some of the smaller alkenes in this study, i.e., for ethene,[13,26−28] propene,[13,26−29] and 1-butene,[28] and we extend these studies to our full set of alkenes and alkynes. It is noteworthy that no experimental or theoretical investigations have been published for HCl addition to alkynes in the gas phase.

For the 24 molecules listed in Table 1, activation energies were computed by means of density functional theory as outlined in the Computational Section. For the three molecules for which experimental values are known, i.e., ethene, propene, and 2-methylpropene, the chosen level of theory gives energies in near agreement with experiments and reproduces the variations in activation energies.[13,14] All computed activation energies are summarized in Tables 2 and 3. Whenever several conformers are possible, only the most stable conformer is used in the calculation. Moreover, to find the most likely transition-state geometry, several possible angles of attack from HCl on the unsaturated bond have been explored.

Table 2. Activation Energies (E_a) and Enthalpies of Protonation (ΔH) of Alkenes, in eV

molecule	atom[a]	E_a[b]	ΔH_{calcd}[b]	ΔH_{exp}
ethene		1.62	−7.06[d]	−7.05[c]
propene	C1	1.36	−7.73	−7.73[h]
	C2	1.69		
1-butene (*skew*)[e,f]	C1	1.28	−7.93	
	C2	1.67		
trans-2-butene	C2	1.43	−7.83[d]	−7.74[c]
1-pentene (*i*)[e,f]	C1	1.28	−8.08	
	C2	1.67		
trans-2-pentene (*skew*)[e,f]	C2	1.37	−7.92	
	C3	1.41		
1-hexene (*I*)[e,f]	C1	1.28	−8.15	−8.35[c]
	C2	1.67		
trans-2-hexene (I)[e,f]	C2	1.36	−8.06	
	C3	1.41		
trans-3-hexene (+ac+ac)[e,f]	C3	1.35	−7.98[d]	
1-heptene (*anti*)[e,g]	C1	1.27	−8.06	
	C2	1.67		
styrene	C1	1.23	−8.72	−8.70[c]
	C2	1.76		
4-methylstyrene	C1	1.17	−8.97	−8.93[c]
	C2	1.77		

[a]Site of H addition. [b]See Section 2 for computational details. [c]Ref 30. [d]Bridged structure. [e]Corresponds to one of the most stable conformers. [f]Ref 20. [g]See Supporting Information. [h]Ref 31.

Table 3. Activation Energies (E_a) and Enthalpies of Protonation (ΔH) of Alkynes, in eV

molecule	atom[a]	E_a[b]	ΔH_{calcd}[b]	ΔH_{exp}[c]
ethyne		1.78	−6.69[d]	−6.65
propyne	C1	1.49	−7.60	−7.75
	C2	1.81		
1-butyne	C1	1.40	−7.79	
	C2	1.77		
2-butyne	C2	1.54	−7.82[d]	−8.04
1-pentyne (*gauche*)[e,f]	C1	1.38	−7.84	
	C2	1.77		
2-pentyne	C2	1.45	−7.92[d]	−8.40
	C3	1.51		
1-hexyne (*aa*)[e,g]	C1	1.39	−8.00	−8.29
	C2	1.77		
2-hexyne (*anti*)[e,g]	C2	1.45	−8.01	−8.35
	C3	1.51		
3-hexyne	C3	1.42	−8.01[d]	
1-heptyne (*aaa*)[e,h]	C1	1.39	−8.03	
	C2	1.76		
ethynylbenzene	C1	1.31	−8.64	−8.62
	C2	1.82		
4-ethynyltoluene	C1	1.23	−8.88	−8.84
	C2	1.81		

[a]Site of H addition. [b]See Section 2 for computational details. [c]Ref 30. [d]Bridged structure. [e]Corresponds to one of the most stable conformers. [f]Ref 19. [g]Ref 20. [h]See Supporting Information.

Figure 2 shows the optimized transition-state geometries of Markovnikov (a) and anti-Markovnikov (b) addition to 1-butene, as well as addition to the nonterminal double bond in *trans*-2-butene (c). The optimized transition-state geometries for the corresponding alkynes are illustrated in Figure 3. In general, the alkynes have been found to be more perturbed in

dx.doi.org/10.1021/jo301627d | J. Org. Chem. 2012, 77, 10105−10117

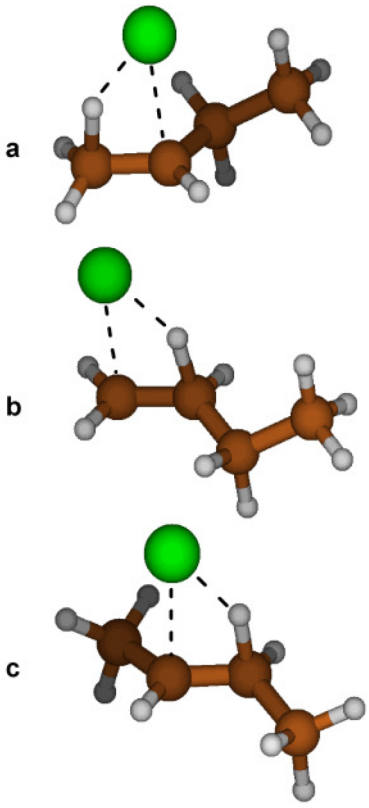

Figure 2. The optimized transition state geometries of the Markovnikov (a) and anti-Markovnikov (b) addition of HCl to 1-butene, and nonterminal HCl addition to trans-2-butene (c).

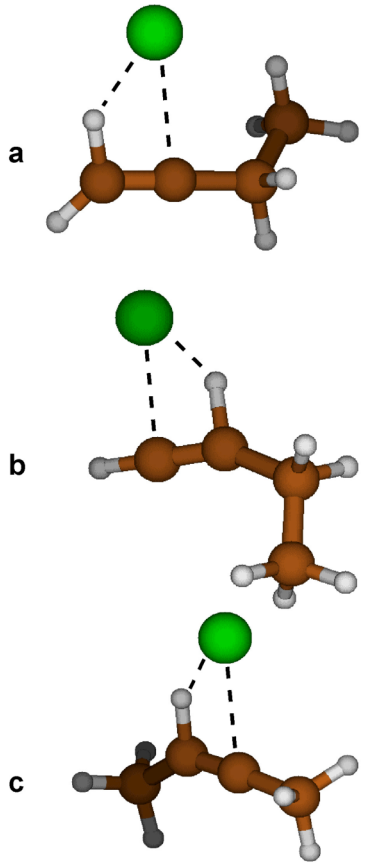

Figure 3. The optimized transition state geometries of the Markovnikov (a) and anti-Markovnikov (b) addition of HCl to 1-butyne, and nonterminal HCl addition to 2-butyne (c).

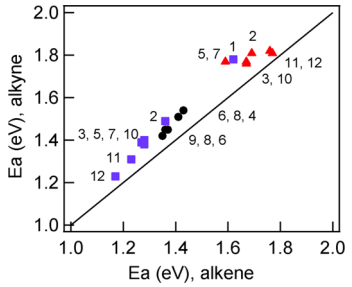

Figure 4. Computed activation energies (E_a) for HCl addition to alkynes plotted against the corresponding alkene activation energies. The Markovnikov reactions are shown with blue squares, whereas anti-Markovnikov additions are indicated by red triangles, and nonterminal with black circles. A 1:1 line is included to guide the eye. See Table 1 for identification of compounds.

the transition state compared to their ground-state geometries, than have the alkenes.

Altogether, 42 addition reactions to alkenes and alkynes have been considered. The compounds are either symmetrically or unsymmetrically substituted about the reactive π bond. Of the latter kind, 7 alkenes follow the pattern $H_2C{=}CHR$, i.e., the two carbon atoms in the double bond differ in the number of hydrogen atoms, and hence the two possible directions of HCl addition may be classified as Markovnikov or anti-Markovnikov according to the original formulation of Markovnikov's rule. We will adhere to the classical use of these terms. From Tables 2 and 3, for these as well as the corresponding alkyne reactions, Markovnikov addition is greatly favored over the alternative direction of addition. The strongest regioselectivity by far is found in the aromatic molecules, displaying very low barriers to Markovnikov addition and correspondingly, the highest barriers to anti-Markovnikov addition.

For *trans*-2-pentene and *trans*-2-hexene the asymmetry of the double bonds is small in the sense that all doubly bonded carbons are attached to one and only one alkyl group. Consistent with this, the difference in activation energy between the two directions of HCl addition is only about 0.05 eV, yet consistently favoring halogen addition to the carbon attached to the longer alkyl moiety. A similar pattern is seen for addition to 2-pentyne and 2-hexyne.

In Figure 4, the activation energies of the alkynes are plotted against the corresponding alkene energies. All points are found above the 1:1 line, indicating that activation energies for the alkenes are systematically lower than those for the corresponding alkynes. Evidently, there is strong correlation between reactivities within each pair of structurally similar alkene and alkyne. However, for the anti-Markovnikov reactions substituent effects are small, as seen from the clustering of points (red triangles) at higher activation energies. A best-fit correlation line, disregarding points for the anti-Markovnikov additions, has a slope of 1.16 with a squared correlation coefficient, R^2, of 0.97. This slope indicates that substituents influence the activation energies of alkynes more than the corresponding alkenes.

3.2. Enthalpies of Protonation. In this section, we will investigate enthalpies of protonation (the negative of the proton affinity), including only Markovnikov directions in the case of unsymmetrical molecules. Since experimental values for

dx.doi.org/10.1021/jo301627d | J. Org. Chem. 2012, 77, 10105−10117

the enthalpy of protonation are available for only a minority of the compounds in Table 1, we use the highly reliable G3 method to obtain a set of values that are homogeneous and of high quality.[25] The accuracy of the resulting values is addressed in the Supporting Information. Experimental and calculated values are summarized in Table 2 for the alkenes and Table 3 for the alkynes.

The calculated enthalpies of protonation for the alkynes are plotted against those of the corresponding alkenes in Figure 5.

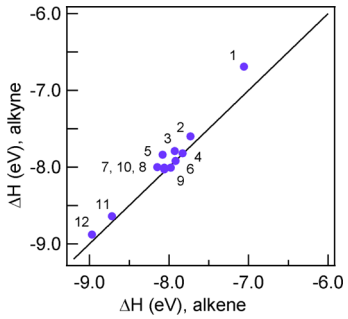

Figure 5. Computed enthalpies of protonation (ΔH) of alkynes plotted against the corresponding alkene predictions using the G3 method. Only points for Markovnikov addition are plotted. The 1:1 line has a slope of 1 and an intercept of 0. See Table 1 for identification of compounds.

In general, the alkynes have similar or slightly less negative enthalpies than do the corresponding alkenes. With the exception of the ethyne/ethene point with a ΔH of about −7 eV for ethene, most of the points are close to the 1:1 line, suggesting small differences in reactivity between double and triple bonds. A best-fit line for ΔH in Figure 5 has a slope of 1.10 with an R^2 of 0.96. The deviation of the ethyne/ethene point is due to the electron-poor character of the triple bond in ethyne. If this point is omitted, the slope changes to 0.97 with R^2 = 0.96.

The slope of the alkyne/alkene correlation for ΔH may now be compared with the corresponding quantity for activation energies for addition of HCl as shown in Figure 4. The slope of 1.16 for E_a, puts the enthalpy of protonation into better agreement with observations for the acid-catalyzed hydration reactions mentioned in the Introduction, than with gas-phase activation energies. This is as expected since the ionic characters of the two model reactions are quite different.

3.3. Carbon 1s Ionization Energies. As outlined in the Introduction, core-level ionization, which introduces a positive charge at a specific, localized sites in a molecule, provides a useful probe of the electronic structure and in particular the nucleophilic character of unsaturated molecules. Carbon 1s photoelectron spectra have been obtained for the complete set of molecules in Table 1, with representative examples included in Figure 6. The photoelectron spectra of the molecules not shown in Figure 6, 1-butyne, 3-hexyne, 1-heptene, 1-heptyne, 4-methylstyrene, and 4-ethynyltoluene, are presented as Supporting Information. Details of the experimental procedures are given in Appendix A.1.

Each spectrum has been analyzed in terms of accurate theoretical line shape models prepared for each unique carbon atom in each of the molecules and superimposed on the spectra as demonstrated in Figure 6. Details of the data analysis and the construction of line shape models are given in Appendix A.2. This procedure has allowed a complete set of C1s ionization

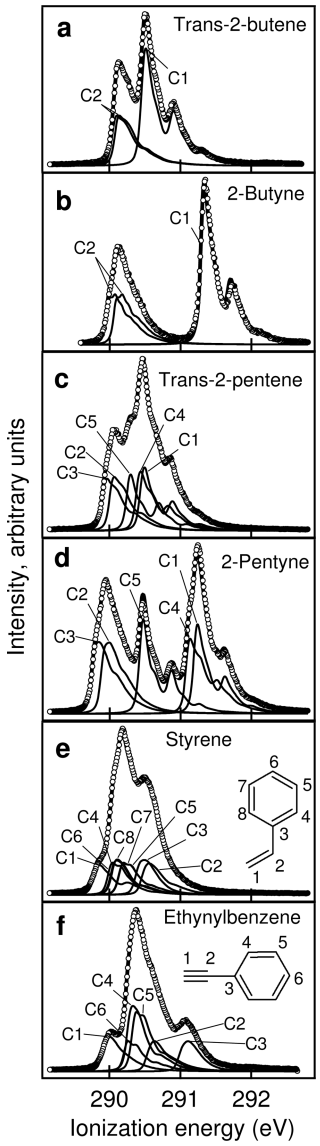

Figure 6. The carbon 1s photoelectron spectra of selected pairs of alkenes and alkynes, including symmetrical (*trans*-2-butene, 2-butyne), unsymmetrical (*trans*-2-pentene, 2-pentyne), as well as aromatic (styrene, ethynylbenzene) molecules. The circles represent the experimental spectrum, the thick solid line the overall theoretical spectrum, and the thin solid lines the theoretical atom-specific line shape profiles.

energies to be obtained for both alkenes and alkynes as listed in Tables 4 and 5, respectively. Also included for comparison are results for ethene[32] and propene,[14] as well as for ethyne[32] and propyne.[33] The values given in the tables are adiabatic ionization energies, i.e., the energy needed to produce the core-ionized ion in its vibrational ground state. The uncertainty of the ionization energies is approximately that of the ionization energy of the calibrant, about 30 meV.[32] The chemical shifts have uncertainties smaller than this, possibly in the 10−15 meV range.[17] In addition to the ionization energies presented in Tables 4 and 5, we make use of C1s energies published elsewhere. These include 1-pentyne from ref 19, and 1-butene, 1-pentene, *trans*-2-pentene, 1-hexene, 1-hexyne, *trans*-2-hexene, 2-hexyne, and *trans*-3-hexene from ref 20.

Some of the molecules listed in Table 1 may possess a number of conformers, and these properties have been explored

dx.doi.org/10.1021/jo301627d | J. Org. Chem. 2012, 77, 10105−10117

Table 4. Experimental Adiabatic Carbon 1s Ionization Energies of the Alkenes, in eV

molecule	atom	ionization energy
ethene		290.695[a,c]
propene	C1	290.136[b]
	C2	290.612[b]
	C3	290.671[b]
trans-2-butene	C1,4	290.498
	C2,3	290.108[c]
1-heptene	C1	289.926
	C2	290.370[d]
	C3	290.318[d]
	C4	290.140[d]
	C5 (*anti*)	290.132
	C6 (*anti*)	290.246[d]
	C7 (*anti*)	290.290[d]
	C5 (*skew*)	290.004[d]
	C6 (*skew*)	290.198[d]
	C7 (*skew*)	290.244[d]
styrene	C1	289.786
	C2	290.465
	C3	290.383
	C4	290.034
	C5	290.150
	C6	290.002
	C7	290.156
	C8	290.043
4-methylstyrene	C1	289.642
	C2	290.393
	C3	290.196
	C4	289.861
	C5	289.903
	C6	290.079
	C7	289.923
	C8	289.918
	C9	290.444

[a]From ref 32. [b]From ref 14. [c]Average of vibronic components. [d]Linked to C5 (*anti*) by the MP4SDQ/TZP shift. See Supporting Information for details.

Table 5. Experimental Adiabatic Carbon 1s Ionization Energies of the Alkynes, in eV

molecule	atom	ionization energy
ethyne		291.128[a,c]
propyne	C1	290.226[b]
	C2	290.778[b]
	C3	291.610[b]
1-butyne	C1	290.057
	C2	290.554
	C3	291.410
	C4	290.673
2-butyne	C1	291.291
	C2	290.012[c]
2-pentyne	C1	291.229
	C2	289.919
	C3	289.792
	C4	291.120
	C5	290.462
3-hexyne	C1	290.442
	C2	291.086
	C3	289.726[c]
1-heptyne	C1	289.945
	C2	290.495[d]
	C3	291.131
	C4	290.390[d]
	C5 (*AAA*)	290.284[d]
	C5 (*GAA*)	290.110
	C6 (*AAA*)	290.347[d]
	C6 (*GAA*)	290.263[d]
	C7 (*AAA*)	290.362[d]
	C7 (*GAA*)	290.284[d]
ethynylbenzene	C1	289.926
	C2	290.554
	C3	291.009
	C4	290.290
	C5	290.360
	C6	290.248
4-ethynyltoluene	C1	289.775
	C2	290.392
	C3	290.791
	C4	290.144
	C5	290.079
	C6	290.259
	C7	290.564

[a]From ref 32. [b]From ref 33. [c]Average of vibronic components. [d]Linked to C5 (*GAA*) by the MP4SDQ/TZP shift. See Supporting Information for details.

using XPS in combination with theory.[19,20] In the following, we consider only the unsaturated carbon atoms, and for practical reasons we use chemical shifts in the C1s energies relative to ethyne, which has the highest ionization energy of the molecules studied here.

In general, C1s ionization energies are influenced by effects of electronegativity, polarizability, and, for unsaturated compounds, by resonance. The general features of the spectra presented here may be understood from the higher electronegativity of the ethynyl group compared to ethenyl and the accompanying charge transfer due to resonance by hyperconjugation,[13,19,33] illustrated in Scheme 2 for alkyl-substituted alkenes. Similar structures may be drawn for the aromatic molecules.

In molecules where the double or triple bond is located terminally, resonance structure I in Scheme 2 leads to transfer of negative charge from carbon 3 to carbon 1. From this, carbon 1 is expected to have the lowest core-ionization energy, while carbon 3 is expected to have the highest. The effect of this resonance has been discussed previously for propene[14] and propyne[33] and will be considered in more detail at the end of the paper when substituent effects are addressed.

Scheme 2

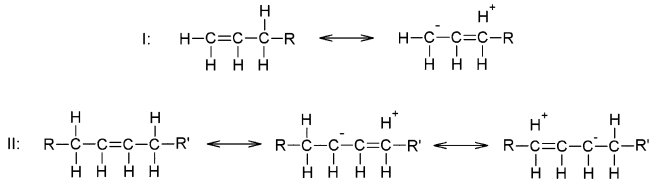

In cases where the double or triple bond is located nonterminally (II in Scheme 2), charge transfer occurs to both unsaturated carbons. As a result, large shifts are observed between the unsaturated carbons and the adjacent atom, see Figure 6. As an example, the C1−C2 shifts for *trans*-2-butene and 2-butyne are 0.34 and 1.28 eV, respectively. The larger

dx.doi.org/10.1021/jo301627d | J. Org. Chem. 2012, 77, 10105−10117

magnitude of the shift in 2-butyne suggests that the charge transfer is larger in the triply bonded system than in the doubly bonded one; this difference presumably arises because there are two π orbitals on the alkyne moiety that can participate in hyperconjugation, whereas for the alkenes there is only one.

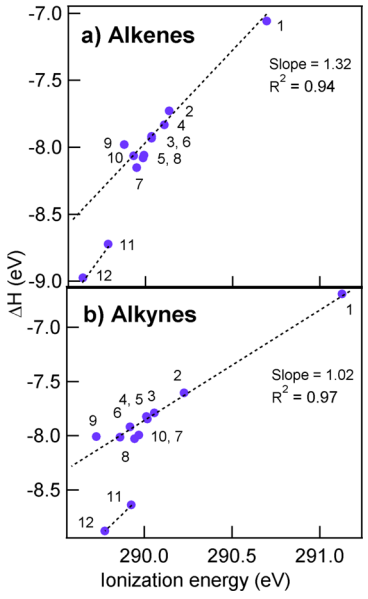

Figure 7. Computed enthalpies of protonation (ΔH) of alkenes (a) and alkynes (b) plotted against carbon 1s ionization energies. Only Markovnikov additions are considered, and the least-squares fit lines do not include the aromatic molecules. See Table 1 for identification of compounds.

3.4. Comparison of Enthalpies of Protonation and C1s Ionization Energies. In Figure 7, the enthalpy of protonation is plotted against C1s energies for both alkenes and alkynes. The data points fall into two groups, one for the alkyl and one for the aryl substituents. The slopes are close to 1, although slightly larger for alkenes than for alkynes.

In the molecules with alkyl substituents, the energies involved for protonation and core ionization are similarly affected by the substituents despite the difference between the two processes. Turning to the molecules with aryl substituents, an additional source of stabilization of the protonated molecules found neither in the protonated molecules with alkyl substituents nor in in the corresponding core-ionized species, is evident. The additional hydrogen introduced in the protonated species opens an opportunity for extending the aromatic π system through a π-symmetry combination of 1s orbitals on the two hydrogens above and below the molecular π-system, as illustrated in Figure 8 for styrene (a) and ethynylbenzene (b). No such orbital is available for core ionization, making the effect of charge redistribution through resonance in the π system substantially larger for protonation than for core ionization. This difference has been noted earlier for processes taking place in the aromatic ring itself,[15,34,35] but is significantly larger here (about 0.5 eV) than was previously observed (about 0.2 eV).

3.5. Comparison of Gas-Phase Activation Energies and C1s Ionization Energies. In Figure 9 activation energies for addition of HCl are plotted against C1s ionization energies, for alkenes (top) and alkynes (bottom) separately. Although there is a certain overall correlation between the two

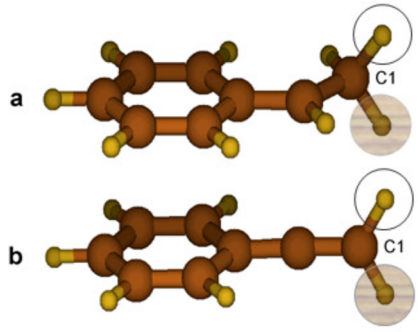

Figure 8. The optimized structure of styrene (a) and ethynylbenzene (b) with a proton added at C1. A π-symmetry combination of H1s orbitals is indicated.

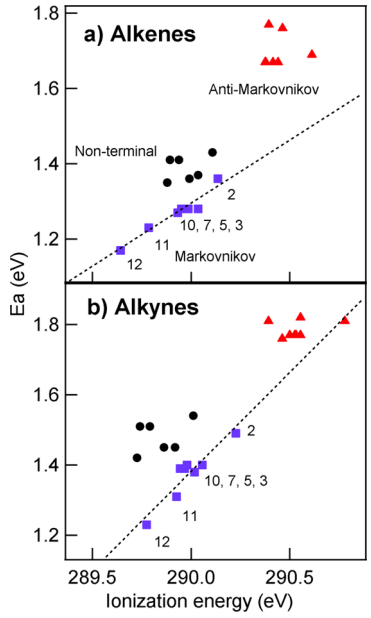

Figure 9. Computed activation energies (E_a) of HCl additions plotted against the carbon 1s ionization energies of alkenes (a) and alkynes (b). The red triangles represent the anti-Markovnikov values, the black circles are the values of the nonterminal unsaturated bond, the blue squares the Markovnikov values, and the dotted lines the Markovnikov least-squares fit lines. See Table 1 for identification of compounds.

observables with R^2 of 0.87 and 0.78, respectively, there is also considerable scatter. The data may most conveniently be discussed in terms of three subsets: Markovnikov and anti-Markovnikov additions to terminal bonds, respectively, and addition to nonterminal bonds. There is an obvious rough correlation, in that for the C2 carbons in the 1-alkene/alkynes, which correspond to the anti-Markovnikov site (and high activation energies), all of the C1s ionization energies are greater or equal to 290.38 eV. By contrast, the ionization energies of the C1 carbons in these compounds, which correspond to the Markovnikov site, are all less than or equal to 290.23 eV. For anti-Markovnikov addition to C2 and for reaction at the nonterminal unsaturated bonds, there is essentially no correlation between the activation energies and the C 1s ionization energies. For the nonterminal molecules the lack of correlation appears to be largely caused by differences in the geometric relaxation associated with core ionization and activation by HCl, respectively. This point is discussed in more detail below.

dx.doi.org/10.1021/jo301627d | J. Org. Chem. 2012, 77, 10105−10117

For Markovnikov addition to terminal double and triple bonds, the correlation between C1s ionization energies and activation energies is positive and quite strong as evident from a squared correlation coefficient of 0.91 for the combined alkene plus alkyne set. Best-fit lines to the separated alkene and alkyne sets as shown in Figure 9, have slopes of 0.34 and 0.55, respectively. Such slopes are expected to be less than 1 since the activation energy is less sensitive to substituent effects than is the ionization energy. This may be understood in part from the difference in electrostatic energy between adding a positive charge by core ionization and bringing the positive end of a dipole close to the reactive site. In addition to this initial-state effect, there is a difference in relaxation energy for the two processes. While the ion/induced-dipole interaction, which stabilizes the final state in the ionization process, falls off as $1/R^4$, the activation energy involves a dipole/induced-dipole interaction, which falls off as $1/R^6$. The activation energies will thus be less sensitive to the size of the molecule than will the ionization energies. In addition, the HCl dipole has less overall electrostatic and polarizing effect than the core charge, implying that polarization effects will overall be less for activation energies than for ionization.

The slopes of the best-fit lines between E_a for Markovnikov addition and C1s energies are much lower than those found between protonation enthalpies and C1s energies (which are close to 1, as indicated in Figure 7). This difference makes it possible to use activation energies and C1s energies in combination to judge the polarity in the transition state of an electrophilic reaction. In solution, the transition states may be characterized as a three-center structure where screening from solvent molecules is likely to favor a high degree of ionicity in the initial electrophilic attack, as was indicated in eq 1. In this case, this transition state would more closely resemble the protonated molecule, and, hence, these activation energies are expected to correlate with enthalpies of protonation. In contrast, the transition states in the gas-phase addition have a pronounced four-center character, as shown in Figures 2 and 3, thus having less of a resemblance to the protonated reactant both structurally and energetically.

The deviation of points from the correlation lines in Figure 9 will now be considered in some detail for internal, i.e., nonterminal, double and triple bonds. In the figure, these are represented by filled circles, and, as noted, correlation between core-level shifts and activation energies is close to zero in this case. In order to explore this result further, the activation energies were plotted against theoretical rather than experimental core-level shifts, albeit with little change. Next, E_a was plotted against computed vertical shifts in C1s energies, i.e., ionization energies obtained in the frozen geometries of the neutral molecules. Now the squared correlation coefficient changes from $R^2 = 0.07$ to 0.20. Finally, the theoretical shift data were recalculated using an artificial geometry for the core-ionized molecule extracted from the corresponding transition-state structure, just leaving out HCl. When activation energies are plotted against the new geometry-corrected shifts, R^2 reaches a value of 0.91 based on 8 points. Apparently, the geometric relaxation that takes place following core ionization at an internal double or triple bond is energetically important and quite different from the geometry change that takes the reacting molecule to the transition state. This may be verified by inspection of transition-state geometries for alkynes and alkenes, such as drawn for 1-butene/*trans*-2-butene and 1-butyne/2-butyne in Figures 2 and 3. In particular for alkynes the change in geometry from a linear core-hole state to a bent transition state is expected to reduce the resonance contribution to the relaxation energy substantially.

3.6. Comparison of C1s Chemical Shifts. We now compare the experimental C1s ionization energies of the carbons in terminal alkenes with the corresponding alkyne values, cf. Figure 10a. The data points for the aliphatic

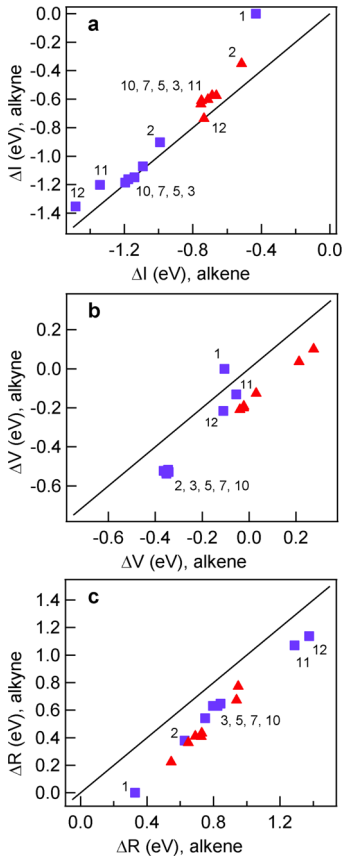

Figure 10. The chemical shift relative to ethyne from experimental C1s ionization energies, ΔI (a), and the contributions to the shift ΔV (b) and ΔR (c) of alkynes with a terminal triple bond plotted against the corresponding alkenes, in eV. The blue squares represent C1s shifts at the Markovnikov position (C1), and red triangles the anti-Markovnikov position (C2). The solid lines have a slope of 1 and intercept of 0. See Table 1 for identification of compounds.

molecules with four or more carbon atoms are located on the 1:1 line, i.e., with essentially the same core-ionization energies for corresponding double and triple bonds. For molecules with two and three carbon atoms as well as for aromatic compounds, the data points are displaced to higher C1s energy for the alkyne compared to the alkene in the pair.

In order to explore this finding closer, we resolve the chemical shift, ΔI, into two contributions; ΔV, which one may think of as the effect of the electric potential at the core of the carbon and is defined by the ground-state charge distribution, and ΔR, which is the effect of electronic and geometric relaxation in the final state. These quantities, illustrated in Figure 10b,c, are connected[14,33] by the relationship $\Delta I = \Delta V - \Delta R$. Details on obtaining ΔV and ΔR are given in Appendix A.3 and as Supporting Information.

In Figure 10b,c, we see that the points for ΔV and those for ΔR are systematically displaced from the reference lines by about 0.2 eV. Since these quantities appear with opposite signs

dx.doi.org/10.1021/jo301627d | J. Org. Chem. 2012, 77, 10105−10117

in ΔI, shifts in ionization energies between corresponding alkynes and alkenes are small, as is seen in Figure 10a. Exceptions to this trend include (i) the aromatic compounds, which show additional large relaxation effects for the alkene compared to the alkyne, and (ii) ethene/ethyne, which is the only pair for which the potential term, ΔV, is higher for the alkyne than for the alkene. This underscores the electron deficiency of the triple bond in ethyne compared to the other alkynes. Moreover, since we use ethyne as a reference compound, this leads to the displacement of all of the other data points in Figure 10b below the 1:1 line. The effect of substituents on values of ΔI, ΔV, and ΔR is further discussed in the next section and in Appendix A.4.

3.7. Substituent Effects. *3.7.1. Activation Energies and C1s Ionization Energies.* The literature of acid-catalyzed hydration reactions[7] indicates that the triple bond is more sensitive to substituents than is the double bond. The slope of the correlation found for E_a in Figure 4 is consistent with this view. The effect of the substituent will now be investigated by considering the variation in activation energies and C1s ionization energies with substituents, relative to parent molecules ethene and ethyne.

In Figure 11, the energies of the Markovnikov addition are plotted as a function of alkyl and aryl substituents on a terminal

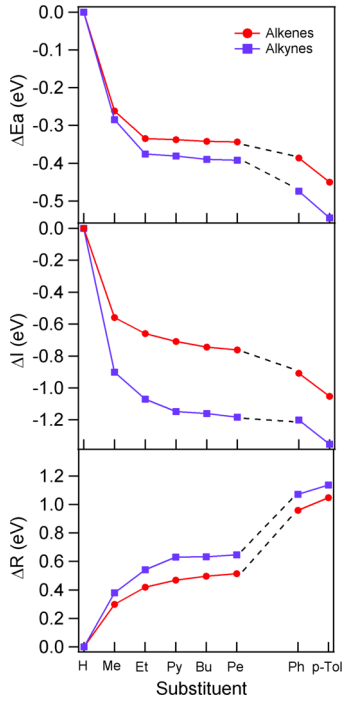

Figure 11. Shifts in activation energies, ΔE_a, carbon 1s ionization energies, ΔI, and final-state relaxation energies, ΔR, plotted against the substituent. The alkene and alkyne values are plotted relative to that of ethene and ethyne, respectively, and show Markovnikov HCl addition to terminal alkenes and alkynes, as well as C1s ionization and relaxation at C1 to the same set of molecules.

unsaturated bond. One of the most striking features of the figure is that the shifts in activation energy (ΔE_a) and ionization energy (ΔI) both decrease smoothly with increasing size of the alkyl substituent. The decrease is largest for the methyl group and then the effect levels off with increasing chain length. This behavior may be understood from the combined effects of hyperconjugation and polarizability. The first is more pronounced for the shorter chains, the second increases with substituent size, but saturates as the chain growth takes place further away from the unsaturated bond. The effect of polarizability has been noted earlier for the linear alkanes.[36]

A second feature of Figure 11 is the influence of the aryl groups which lowers both ionization and activation energies more than the alkyl substituents. The influence of the remote methyl group in *p*-tolyl is notable. This effect is attributed to enhanced resonance due to the aromatic system and the electron-donating property of the methyl group in the para position.

The third feature of the figure addresses the differences between the alkynes and alkenes. It is seen that the effect of substituents is more pronounced for the triple bonds than for the double bonds, especially for ionization energies. This may be understood from the larger electronegativity of the ethynyl group, but also from differences in charge redistribution of the final state, ΔR. Values of ΔI, ΔV, and ΔR, relative to the parent compounds, are summarized in Table 5 of the Supporting Information. In the lower part of Figure 11, ΔR is plotted as a function of the substituents involved. It is apparent that the values increase smoothly with the size of the alkyl groups as expected from the relationship between polarizability and molecular size. We can also anticipate that there is contribution from resonance and hyperconjugation similar to the charge delocalization shown in Scheme 2. The contribution from ΔV is significant, making up 30−40% of ΔI for alkenes, and 40−50% for alkynes, but is approximately independent of size. For the aryl substituents, by far the largest contribution to ΔI comes from ΔR, which is much more significant for these substituents than it is for alkyl substituents.

3.7.2. Additivity of Substituent Effects. A convenient way of summarizing substituent effects is to use linear additivity correlations. The model assumes that the total effect is equal to the sum of independent effects of the individual substituent.[15,34,35] Using substituted alkynes as an example, we recognize that each alkyne has the formula $Y_\alpha C_\alpha C_\beta Y_\beta$, where Y_α and Y_β can be H, CH_3, an alkyl group R larger than methyl, or an aryl group. If we ignore the aromatic groups, then we can describe any alkyne by specifying, $(\alpha_{CH_3},\alpha_R,\beta_{CH_3},\beta_R)$, where each α or β gives the number of substituents of the indicated type attached to $C_\alpha C_\beta$, respectively. Each α or β as well as the sums, $\alpha_{CH_3} + \alpha_R$ and $\beta_{CH_3} + \beta_R$, must be either zero or one. Ethyne, for example, is specified by (0,0,0,0). We consider C_α as the reactive carbon of interest. We can then make the following Ansatz for the activation energies, E_a:

$$E_a = \text{constan} + a\alpha_{CH_3} + b\alpha_R + c\beta_{CH_3} + d\beta_R \qquad (2)$$

The parameters a, b, c, and d are determined from a least-squares fitting of all the activation energies of the alkynes. A similar expression can be written for the alkenes, and a constant term is also included to allow for the difference between ethene and ethyne.

The activation energies for both alkynes and alkenes are well described by such an additivity model. For the alkynes, R^2 = 0.9985 and the rms deviation is 0.01 eV. For the alkenes, the corresponding quantities are 0.9994 and 0.006 eV. The parameters from the alkyne and alkene fits, both for the effect of methyl, alkyl and aryl substituents on the activation energies, are summarized in Table 6.

The offset of the alkyne data from the alkene data is seen in the difference of 0.15 eV between the two intercepts

dx.doi.org/10.1021/jo301627d | J. Org. Chem. 2012, 77, 10105−10117

Table 6. Additivity Coefficients of the Alkynes and Alkenes Summarized in Table 1, for the Effect of Methyl, Alkyl or Aryl Substituents on the Activation Energies, in eV[a]

substituent	position	alkynes	alkenes
CH_3	α	0.052 (6)	0.081 (4)
	β	−0.266 (6)	−0.259 (3)
R	α	0.013 (6)	0.059 (4)
	β	−0.364 (6)	−0.331 (4)
Ph	α	0.148	0.061
	β	−0.382	−0.449
Tol	α	0.158	0.051
	β	−0.442	−0.529
	Constant[b]	1.759 (6)	1.612 (4)

[a]Uncertainties in the last digit are shown in parentheses. For the aryl substituents the number of measurements is equal to the number of parameters. [b]Constant of the regression.

(constants). In general, the parameters for the alkynes are very similar to those for the alkenes. For the replacement of a hydrogen atom on the carbon of interest by an alkyl group there is an increase in the activation energy. This is consistent with the higher electronegativity of the alkyl groups relative to hydrogen, which leads to more positive charge at this carbon, making it less receptive to attack by the hydrogen in HCl. A much larger effect of opposite sign is seen when the alkyl group is added in position β to the carbon of interest. Hyperconjugation leads to negative charge being transferred to C_α, with an accompanying lowering of the activation energy for Markovnikov addition. A similar trend is observed for the effect of aryl substituents on the activation energies. However, as can be seen in Table 6, the β effect is clearly larger for the aryl groups than it is for the alkyl groups.

Similar additivity correlations have been considered for ΔI shifts as well as for shifts in ΔV and ΔR separately, to explore substituent effects from these quantities. It is found that both ΔI and ΔV are reasonably well described by an additivity model, whereas ΔR is not. Further details on these results are reported in Appendix A.4.

4. CONCLUSIONS

Electrophilic addition to carbon−carbon double and triple bonds has been investigated in the gas phase for a set of twelve alkenes and the corresponding alkynes. The relative chemical reactivity has been probed by calculated enthalpies of protonation and activation energies for HCl addition and compared with experimental carbon 1s ionization energies. In each of these processes, a positive charge is added to a specific site of the unsaturated bond and provides information on chemical effects, even if the energies involved are quite different. The chemical effects considered here are conjugation by the neighboring alkyl and aryl groups as well as the polarization of the substituents. The reactivity of the alkene is found to be similar to or larger than that of the corresponding alkyne for protonation and HCl addition. The same trend is found for relative values of C1s energies for terminal unsaturated bonds, but not for internal π-systems.

For alkyl-substituted compounds, enthalpies of protonation and C1s energies are well correlated with slopes of about 1, indicating that the energies involved for protonation and core ionization are similarly affected by the substituents. However, the aromatic systems are found at lower enthalpies clearly displaced from the line of the alkyl substituents. Enthalpies of protonation for the alkyl groups and the aryl groups compared to core-ionization energies provide insight into the π-donor abilities of the two systems.

For activation energies, both alkyl- and aryl-substituted molecules correlate reasonably well with C1s energies provided that the charge addition is restricted to Markovnikov addition to a terminal multiple bond. The slopes are significantly lower than 1, indicating that the transition-state energy is less sensitive to substituent effects than is the ionization energy. However, the activation energies for anti-Markovnikov addition and addition to nonterminal bonds are all found at higher energies relative to the Markovnikov line. The offset from the line may be explained by differences between the geometries of the transition state and those of the core-hole state, which influence terminal and nonterminal bonds differently.

Substituent effects are compared for alkenes and alkynes by using both activation energies and C1s energies. These are found to be largest for the triple bonds, in agreement with experimental results obtained from acid-catalyzed hydration reactions. Comparison of ground- and final-state effects exerted by the substituents shows that for alkyl groups the effect of charge donation in the ground state is significant for both series of compounds. For the aryl substituents, by far the largest contribution to the ionization energies comes from final-state effects, which is much more significant for these substituents than it is for alkyl substituents. Substituent effects were summarized using a linear additivity model. The obtained parameters provide additional insight into the effects of alkyl and aryl substituents for both alkynes and alkenes.

APPENDIX

A. Carbon 1s Ionization Energies

A.1. Experimental Section. Carbon 1s photoelectron spectra were recorded for most of the compounds of interest in this work at beamline I411 of the MAX II synchrotron in Lund, Sweden.[37] The photon energy was 330 eV, and the photoelectrons were analyzed in an SES200 electron spectrometer. The total instrumental broadening is represented by a Gaussian distribution with a full width at half-maximum (fwhm) determined from the carbon 1s photoelectron spectrum of carbon dioxide. The CO_2 spectrum also provides calibration of the ionization energy scale.[32] The carbon 1s spectra of 1-butyne and 2-butyne were measured at beamline 10.0.1 at the Advanced Light Source (ALS) in Berkeley, U.S.[38] For the ALS measurements, the instrumental broadening and energy calibration were provided from the argon 2p spectrum for 1-butyne and from the carbon 1s photoelectron spectrum of CF_4 for 2-butyne. The Gaussian widths for the molecules presented in this work range from 60 to 77 meV, and all measurements were made at room temperature (~25 °C).

A.2. Spectral Analysis. For all molecules, the experimental spectrum is decomposed into contributions from the different carbon atoms. For each atom, there is a vibrational profile reflecting the vibrational excitation associated with ionization of that atom. The procedure used is to prepare theoretical line shape models specific to each site of ionization, followed by fitting the line shape profiles to the observed spectrum by least-squares techniques.[39]

Construction of the line shape models involves Franck−Condon analyses of the vibrational profiles associated with each site of ionization. To this end, optimized geometries, vibrational frequencies, and normal modes have been computed for the

neutral and C1s-ionized molecules by means of the B3LYP method and TZP basis as described in Section 2. For the core-ionized carbon atom, the corresponding nitrogen basis was used with all exponents scaled by a common factor of 0.9293, obtained by minimizing the calculated energy of core-ionized methane.[36] The core of the ionized carbon atom was represented by the effective core potential (ECP) of Stevens et al.,[40] scaled to account for only one electron in the 1s shell.[41] Further details of these procedures can be found in refs 19, 20, 36, and 42.

All of the unique carbon atoms of *trans*-2-butene, 1-butyne, 2-butyne, 2-pentyne, and 3-hexyne are well resolved in the carbon 1s photoelectron spectrum. Hence, these spectra are fitted with energies and intensities allowed to vary independently. However, for styrene, 4-methylstyrene, ethynylbenzene, and 4-ethynyltoluene, the shifts between the carbons in the main peaks are relatively small. To ensure that all of the fit parameters are reproducible and reliable, the relevant intensity areas of these carbons are constrained to be the same.

For *trans*-2-butene and 2-butyne the molecular symmetry causes the peaks of the unsaturated carbons to split.[43−46] To account for this effect, the central carbons are represented by two identical vibrational profiles only energy shifted by 36 and 101 meV for *trans*-2-butene and 2-butyne, respectively, obtained by least-squares fitting to the spectra. Such vibrational splittings are estimated reasonably well from orbital energies calculated at the Hartree−Fock level.[47,48] For the molecules considered here, the HF/TZP predictions give 47 and 102 meV, respectively, in good agreement with the experimental values.

In the case of 1-heptene and 1-heptyne, where several conformers contribute significantly to the spectrum, some of the different vibrational profiles are overlapping with very small ionization energy differences. To prevent unreasonable and unphysical fitting results, the relative energy positions are constrained using chemical shifts calculated at the MP4SDQ/TZP level of theory, which has been found to give reasonably accurate predictions of relative C1s ionization energies.[17] Furthermore, the intensity areas of these carbons are constrained to be the same. For carbons that are well separated in energy and have their own defined peaks both energy and intensity are allowed to independently change.

A.3. Ground-State and Relaxation Contributions to Chemical Shifts. To facilitate a more detailed analysis of chemical shifts in C1s ionization energies, it is useful to split the chemical shift, ΔI, into one contribution, ΔV, that may be ascribed to the ground-state charge distribution, and a second term, ΔR, that takes into account electronic and geometric relaxation in the ionized state. These quantities are related through eq 3.[14,33]

$$\Delta I = \Delta V - \Delta R \tag{3}$$

To include both the wave nature of core electrons and the influence of the valence electron correlation on the electrostatic potential, V, two of the present authors[49] proposed to calculate the initial-state contribution to the chemical shift from $\Delta V \approx \Delta U^{\mathrm{VCI}} - (\Delta\varepsilon_c + \Delta U^{\mathrm{HF}})$. In this equation, which is valid in the case of well-localized or close-to-degenerate inner-shell orbitals, $\Delta\varepsilon_c$ is the difference in initial-state core-orbital energies, ΔU the difference in electrostatic energy of a unit positive charge at the nuclei to be compared, and superscripts HF and VCI are the Hartree−Fock and valence-correlated levels of theory, respectively. To compute ΔV, MP2 was used as the valence-correlated level of theory, and the TZP basis was used in both HF and MP2 computations. The core-orbital energies ($\Delta\varepsilon_c$) were computed at the HF/TZP level of theory. ΔR is found by subtracting experimental values of ΔI from ΔV, cf., eq 3. Calculated values of ΔV and ΔR relative to ethyne are given in Tables 3 and 4 of the Supporting Information section.

A.4. Additivity of Substituent Effects from Shifts in ΔI, ΔV, and ΔR. Activation energies of alkenes and alkynes are well described by additivity models. In this section, similar correlations are considered for shifts in ΔI, ΔV, and ΔR. For the ΔV data, both the alkyne and alkene correlations are found to be highly satisfactory. For the alkynes, the correlation coefficient R^2 is 0.997 and the rms deviation of the points from the fit is 0.03 eV. For the alkenes, the corresponding numbers are 0.998 and 0.01 eV. The data from these fits are shown in Table 7.

Table 7. Additivity Coefficients of the Alkynes and Alkenes Summarized in Table 1, for the Effect of Methyl, Alkyl or Aryl Substituents on the ΔV Values, in eV[a]

substituent	position	alkynes	alkenes
CH_3	α	−0.067 (17)	0.134 (7)
	β	−0.518 (11)	−0.262 (7)
R	α	−0.187 (12)	0.077 (7)
	β	−0.502 (12)	−0.244 (7)
Ph	α	0.101	0.380
	β	−0.131	0.049
Tol	α	0.037	0.317
	β	−0.216	−0.006
	constant[b]	0	−0.104 (7)

[a]Uncertainties in the last digit are shown in parentheses. For the aryl substituents the number of measurements is equal to the number of parameters. [b]Constant of the regression.

Several features can be seen in these parameters. First, there is a negative offset of the alkenes relative to the alkynes, reflecting the electron-donating effect of the additional hydrogen atoms on the alkenes. Second, the effect of hyperconjugation is seen in the large values for β_{CH_3} and β_R. These parameters are twice as large for alkynes as for alkenes. The difference between the effect of a methyl group and a larger alkyl group is small. Third, the effect of an alkyl group on the α carbon is positive for the alkenes, as expected, but negative for the alkynes, contrary to expectation. Fourth, the values for the aromatic groups are in accord with the previous discussion.

For the ΔI shifts, however, the correlations are poorer. The ΔI shifts depend on both ΔV and ΔR, and although ΔV is well described by such a model, ΔR is not. ΔR appears to depend primarily on molecular size; the relaxation is larger for R than for CH_3. There is also some correlation with position; a β alkyl group produces more relaxation than does an α alkyl group. Although ΔV does not depend much on the size of the alkyl group, this is not the case for ΔR. For each addition of a carbon atom to the alkyl chain, ΔR increases, although by a smaller amount as the chain gets longer. Thus we cannot expect the model described here to give a complete picture of the relaxation-energy shifts, and consequently, nor of the ionization-energy shifts. As a result, we get an adequate but not excellent model if we try to describe ΔI by additivity. For the alkynes R^2 is 0.975 and the rms is 0.07 eV; for the alkenes, these are 0.978 and 0.04 eV. The parameters describing the

effect of alkyl substitution on the alkenes and alkynes are shown in Table 8.

Table 8. Additivity Coefficients of the Alkynes and Alkenes Summarized in Table 1, for the Effect of Methyl and Alkyl Substituents on the ΔI Values, in eV[a]

substituent	position	alkynes	alkenes
CH_3	α	−0.17 (5)	0.01 (3)
	β	−0.78 (5)	−0.49 (3)
R	α	−0.43 (5)	−0.21 (3)
	β	−0.95 (5)	−0.61 (3)
	Constant[b]	290.98 (5)	290.61 (3)

[a]Uncertainties in the last digit are shown in parentheses. [b]Constant of the regression.

It is useful to note here that for C_α on 1-alkenes and 1-alkynes, the shift in ionization energy is determined by β_{CH_3} and β_R. For both of these, the magnitude is larger for the alkynes than for the alkenes.

■ ASSOCIATED CONTENT

Supporting Information

The −log{k} values from acid-catalyzed hydration reactions, valence ionization energies, carbon 1s photoelectron spectrum of 1-butyne, 3-hexyne, 1-heptene, 1-heptyne, 4-methylstyrene, and 4-ethynyltoluene, a conformational analysis of 1-heptene and 1-heptyne, enthalpies of protonation, ΔI, ΔV, and ΔR values, basis sets, and molecular geometries. This material is available free of charge via the Internet at http://pubs.acs.org.

■ AUTHOR INFORMATION

Corresponding Author

*Phone: +47 5558 3561; fax: +47 5558 9490; e-mail: leif.sathre@kj.uib.no.

Notes

The authors declare no competing financial interest.

■ ACKNOWLEDGMENTS

We are pleased to thank Maxim Tchaplyguine at beamline I411 and the MAX-lab staff for their assistance during the beamtime. A.H., L.J.S. and K.J.B. acknowledge the Nordic Research Board (NORDFORSK), the Norwegian High Performance Computing Consortium NOTUR and the EC Transnational Access to Research Infrastructure Program (TARI).

■ REFERENCES

(1) Carey, F. A.; Sundberg, R. J. *Advanced Organic Chemistry*; 5th ed.; Springer: New York, 2007; p 531.
(2) Mascavage, L. M.; Zhang-Plasket, F.; Sonnet, P. E.; Dalton, D. R. *Tetrahedron* **2008**, *64*, 9357−9367.
(3) Melloni, G.; Modena, G.; Tonellato, U. *Acc. Chem. Res.* **1981**, *14*, 227.
(4) Yates, K.; Schmid, G. H.; Regulski, T. W.; Garratt, D. G.; Leung, H.-W.; McDonald, R. *J. Am. Chem. Soc.* **1973**, *95:1*, 160−165.
(5) Modena, G.; Rivetti, F.; Tonellato, U. *J. Org. Chem.* **1978**, *43*, 1521−1526.
(6) Marcuzzi, F.; Melloni, G.; Modena, G. *J. Org. Chem.* **1979**, *44*, 3022−3028.
(7) Allen, A. D.; Chiang, Y.; Kresge, A. J.; Tidwell, T. T. *J. Org. Chem.* **1982**, *47*, 775.
(8) *NIST Chemistry WebBook*. Available from: http://webbook.nist.gov/chemistry/. See Supporting Information.
(9) Nelson, D. J.; Soundararajan, R. *Tetrahedron Lett.* **1988**, *29*, 6207−6210.
(10) Nelson, D. J.; Cooper, P. J.; Soundararajan, R. *J. Am. Chem. Soc.* **1989**, *111*, 1414−1418.
(11) Nelson, D. J. *Tetrahedron Lett.* **1999**, *40*, 5823−5826.
(12) Nelson, D. J.; Li, R.; Brammer, C. *J. Org. Chem.* **2001**, *66*, 2422−2428.
(13) Sæthre, L. J.; Thomas, T. D.; Svensson, S. *J. Chem. Soc., Perkin Trans. 2* **1997**, 749.
(14) Thomas, T. D.; Sæthre, L. J.; Børve, K. J.; Gundersen, M.; Kukk, E. *J. Phys. Chem. A* **2005**, *109*, 5085.
(15) Myrseth, V.; Sæthre, L. J.; Børve, K. J.; Thomas, T. D. *J. Org. Chem.* **2007**, *72*, 5715−5723.
(16) Mascavage, L. M.; Dalton, D. R. *Trends Org. Chem.* **1993**, *4*, 303−333.
(17) Holme, A.; Børve, K. J.; Sæthre, L. J.; Thomas, T. D. *J. Chem. Theory Comput.* **2011**, *7*, 4104−4114.
(18) Sæthre, L. J.; Børve, K. J.; Thomas, T. D. *J. Electron Spectrosc. Relat. Phenom.* **2011**, *183*, 2−9.
(19) Holme, A.; Sæthre, L. J.; Børve, K. J.; Thomas, T. D. *J. Mol. Struct.* **2009**, *920*, 387−392.
(20) Holme, A.; Børve, K. J.; Sæthre, L. J.; Thomas, T. D. , manuscript in preparation.
(21) Frisch, M. J. et al.; *Gaussian 03, Revision C.02*; Gaussian, Inc.: Wallingford CT, 2004.
(22) Dunning, T. H., Jr. *J. Chem. Phys.* **1971**, *55*, 716.
(23) Raghavachari, K.; Binkley, J. S.; Seeger, R.; Pople, J. A. *J. Chem. Phys.* **1980**, *72*, 650.
(24) McLean, A. D.; Chandler, G. S. *J. Chem. Phys.* **1980**, *72*, 5639.
(25) Curtiss, L. A.; Raghavachari, K.; Redfern, P. C.; Rassolov, V.; Pople, J. A. *J. Chem. Phys.* **1998**, *109*, 7764.
(26) Suresh, C. H.; Koga, N.; Gadre, S. R. *J. Org. Chem.* **2001**, *66*, 6883−6890.
(27) Aizman, A.; Contreras, R.; Galván, M.; Cedillo, A.; Santos, J. C.; Chamorro, E. *J. Phys. Chem. A* **2002**, *106*, 7844−7849.
(28) Ding, Y. L.; Mu, J. R.; Wang, C. H.; Yang, Z. Z. *Int. J. Quantum Chem.* **2011**, *111*, 2778−2787.
(29) Burda, J. V.; Murray, J. S.; Toro-Labbé, A.; Gutiérrez-Oliva, S.; Politzer, P. *J. Phys. Chem. A* **2009**, *113*, 6500−6503.
(30) Hunter, E. P. L.; Lias, S. G. *J. Phys. Chem. Ref. Data* **1998**, *27*, 413.
(31) Brooks, A.; Lau, K.-C.; Baer, T. *Eur. J. Mass Spectrom.* **2004**, *10*, 819−828.
(32) Myrseth, V.; Bozek, J. D.; Kukk, E.; Sæthre, L. J.; Thomas, T. D. *J. Electron Spectrosc. Relat. Phenom.* **2002**, *122*, 57−63.
(33) Sæthre, L. J.; Berrah, N.; Bozek, J. D.; Børve, K. J.; Carroll, T. X.; Kukk, E.; Gard, G. L.; Winter, R.; Thomas, T. D. *J. Am. Chem. Soc.* **2001**, *123*, 10729−10737.
(34) Carroll, T. X.; Thomas, T. D.; Bergersen, H.; Børve, K. J.; Sæthre, L. J. *J. Org. Chem.* **2006**, *71*, 1961−1968.
(35) Carroll, T. X.; Thomas, T. D.; Sæthre, L. J.; Børve, K. J. *J. Phys. Chem. A* **2009**, *113*, 3481−3490.
(36) Karlsen, T.; Børve, K. J.; Sæthre, L. J.; Wiesner, K.; Bässler, M.; Svensson, S. *J. Am. Chem. Soc.* **2002**, *124*, 7866−7873.
(37) Bässler, M.; Forsell, J.-O.; Björneholm, O.; Feifel, R.; Jurvansuu, M.; Aksela, S. *J. Electron Spectrosc. Relat. Phenom.* **1999**, *101−103*, 953−957.
(38) http://www-als.lbl.gov/als/techspecs/bl10.0.1.html.
(39) *Spectral Analysis by Curve Fitting Macro Package SPANCF*. Available from the following: http://www.physics.utu.fi/en/research/material_science/Fitting.html.
(40) Stevens, W. J.; Basch, H.; Krauss, M. *J. Chem. Phys.* **1984**, *81*, 6026.
(41) Karlsen, T.; Børve, K. J. *J. Chem. Phys.* **2000**, *112*, 7979.
(42) Oltedal, V. M.; Børve, K. J.; Sæthre, L. J.; Thomas, T. D.; Bozek, J. D.; Kukk, E. *Phys. Chem. Chem. Phys.* **2004**, *6*, 4254.
(43) Bozek, J.; Carroll, T. X.; Hahne, J.; Sæthre, L. J.; True, J.; Thomas, T. D. *Phys. Rev. A* **1998**, *57*, 157.

(44) Børve, K. J.; Sæthre, L. J.; Thomas, T. D.; Carroll, T. X.; Berrah, N.; Bozek, J. D.; Kukk, E. *Phys. Rev. A* **2000**, *63*, 012506.
(45) Karlsen, T.; Sæthre, L. J.; Børve, K. J.; Berrah, N.; Kukk, E.; Bozek, J. D.; Carroll, T. X.; Thomas, T. D. *J. Phys. Chem. A* **2001**, *105*, 7700.
(46) Myrseth, V.; Børve, K. J.; Wiesner, K.; Bässler, M.; Svensson, S.; Sæthre, L. J. *Phys. Chem. Chem. Phys.* **2002**, *4*, 5937.
(47) Domcke, W.; Cederbaum, L. S. *Chem. Phys.* **1977**, *25*, 189.
(48) Cederbaum, L. S.; Domcke, W. *Chem. Phys.* **1977**, *26*, 169−177.
(49) Børve, K. J.; Thomas, T. D. *J. Electron Spectrosc. Relat. Phenom.* **2000**, *107*, 155−161.